Mem. S.A.It. Vol. 93, 21

Memorie della

High-Energy observations of Stellar-mass Compact Objects: from CVs to the most luminous X-Ray Binaries

T.M. Belloni[1], A. Bazzano[2], P. Casella[3], M. Del Santo[4], R. Iaria[5], N. Masetti[6], S. Mereghetti[7], A. Papitto[3], and L. Zampieri[8]

[1] INAF-Osservatorio Astronomico di Brera, Via E. Bianchi 46, I-23807 Merate, Italy e-mail: tomaso.belloni@inaf.it
[2] INAF-Istituto di Astrofisica e planetologia spaziali di Roma, via Fosso del Cavaliere 100, I-00133, Roma, Italy
[3] INAF-Osservatorio Astronomico di Roma, Via Frascati 33, I-00040, Monte Porzio Catone, Italy
[4] INAF-Istituto di Astrofisica spaziale e fisica cosmica, via Ugo la Malfa 153, I-90146, Palermo, Italy
[5] Dipartimento di scienze fisiche e astronomiche, Università di Palermo, via Archirafi 36, I-90123, Palermo, Italy
[6] INAF-Osservatorio di Astrofisica e Scienza dello Spazio, via Gobetti 101, I-40129, Bologna, Italy
[7] INAF-Istituto di Astrofisica Spaziale e Fisica cosmica, via A. Corti 12, I- 20133 Milano, Italy
[8] INAF-Osservatorio Astronomico di Padova, Vic. Osservatorio 5, I-35122 Padova, Italy

Received: 14 December 2021; Accepted: 19 May 2022

Abstract. This is the report of a project involving the majority of the Italian community working on stellar-mass compact objects, ranging from cataclysmic variables, to magnetars, pulsars, Galactic black-hole and neutron-star binaries and accreting X-ray Sources in external galaxies. The project is based on a large amount of proprietary data from guest-observer programs of most high-energy missions currently operative, plus involvement in additional international proposals and programs for exploitation of archival data. The groups of the project form a full network as there are numerous ongoing collaborations both on observations and theory. Given the space limitations, only selected highlights are presented.

Key words. accretion, accretion discs - stars: black holes - stars: neutron - white dwarfs - binaries - X-rays: binaries

1. Introduction

The category of stellar-mass compact objects comprises three types of collapsed stars: white dwarfs, neutron stars ad black holes.

Nevertheless, the zoo of associated high-energy sources is varied: different classes of cataclysmic variables, isolated neutron stars, magnetars, millisecond, rotation-powered pul-

sars and accreting pulsars, neutron-star binaries, Supergiant Fast X-ray Transients, black-hole binaries, ultraluminous X-ray sources. The INAF community is very active in the study of these objects, with a number of research groups in different institutes throughout the country. These groups constitute a research network that has obtained funding through the ASI-INAF agreement in 2017 to support guest-observer time on all major high-energy facilities. In this paper, we report selected results, by no means exhaustive. The authors are the team leaders of the various groups, who appear on behalf of all participants to the project.

2. Black-hole binaries

The availability of space missions such as NICER, Astrosat and Insight-HXMT allows for detailed study of fast timing variability from Black-Hole Binaries (BHB). In particular, one can study in detail Quasi-Periodic Oscillation (QPO: see Ingram & Motta 2019 for a review). These are divided into classes: of these, type-C QPOs have been associated with relativistic frequencies in the accretion flow, while type-B QPOs are thought to be connected to the emission of relativistic jets. In the recent years, variability studies have been extended to longer wavelength: the detection of signals in the optical and infrared bands allow a more complete characterization of QPOs and can provide a stronger grip on their origin.

2.1. QPOs in the X-ray emission of black-hole binaries

We have performed a detailed timing and spectral analysis of a set of NICER observations of the bright transient MAXI J1348-630 (Belloni et al. , 2020). We selected observations from the brightest part of the 2019 outburst belonging to the Soft-Intermediate State (SIMS) and therefore feature a strong type-B QPO. The oscillation remains at the roughly constant frequency of 4.5 Hz, which allowed us to accumulate an exposure of more than 25 ks at a source count rate that went above 30 kcts/s.

We compute the energy dependence of the fractional rms and the phase lags at the QPO frequency, obtaining high signal-to-noise data and sampling for the first time at energies below 2 keV. The fractional rms increases with energy up to the highest energy bin (10 keV), but is constant below 1.5 keV. The phase lags of type-B QPOs are known to be positive (hard lags soft) and to increase with energy, but until now they were measured only above ∼2-3 keV. This is confirmed in our data, but below 2 keV they start increasing again, reaching almost one radiant below 1 keV. This means that at the QPO frequency the hard photons lead the soft photons. The results can be seen in Fig. 1.

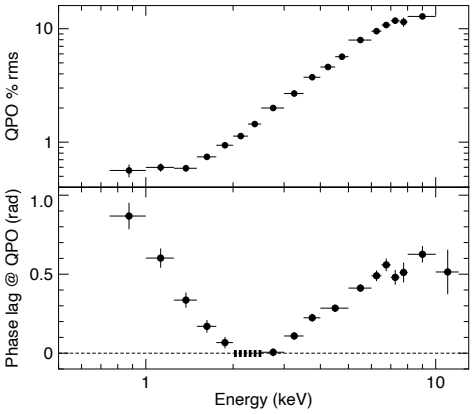

Fig. 1. Top panel: energy spectrum of the QPO fractional rms for the type-B QPO. Bottom panel: corresponding phase lag spectrum at the QPO. The reference energy band is shown by the dashed line.

The energy spectrum from the same observation could be fitted with a standard model for a BHB in the SIMS, consisting of the sum of a disk component, a hard Comptonized component and an iron emission line between 6 and 7 keV. We interpreted the results in terms of a standard Comptonization scenario. In a subsequent publication (Garcia et al. , 2021), we have applied a more complex variable-Comptonization model (Karpouzas et al. , 2020), which allows to fit at the same time the energy spectrum and the timing properties in Fig. 1. We find that two Comptonization regions in the accreting flow can fit remarkably well both spectral and timing data.

The study of low-frequency QPOs (both type-B and type-C) and in particular the lag be-

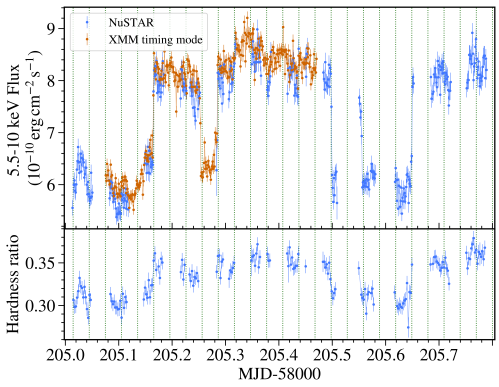

Fig. 2. Light curves and hardness ratio of the NuSTAR and XMM-Newton observation of the late transitions in Swift J1658.2-4242. Vertical lines are drawn every 2761 s.

tween hard and soft photons has been carried forth in a number of other objects as part of an ongoing collaboration with the University of Groningen. We have analyzed the data and applied the Comptonization model to a number of systems, including GRS 1915+105 (Zhang et al. , 2020; Karpouzas et al. , 2021; Méndez et al. , 2021), and MAXI J1535-571 (Zhang et al., submitted; Rawat et al., submitted).

Finally, complex and fast state-transitions from the less bright system Swift J1658.2-4242 were observed with many instruments (XMM-Newton, NuSTAR, Astrosat, Swift, Insight-HXMT and INTEGRAL) and analyzed the quasi-simultaneous data (Bogensberger et al. , 2020). These transitions corresponded to marked changes in the fast timing properties, but what is most important (and puzzling) is that the early transitions were aligned with a very precise clock, taking place at distances that are multiples of 2761 s. In the late transitions, taking place after some time, this period is slightly lower (2610 s, see Fig. 2). It is unclear what can be the physical origin of this period.

2.2. Optical/X-ray variability of the BHB MAXI J1820+070

The optical/X-ray timing analysis of the collaboration covers various topics including the study of magnetars and other isolated NS, transient X-ray binaries, ULXs, and transitional millisecond pulsars. Observations are carried out in the high energy and optical bands, and make also use of optical high time resolution instrumentation available to the team (Aqueye+, IFI+Iqueye; Zampieri et al. 2019).

Here we report an highlight of the results recently obtained on MAXI J1820+070. In 2018 and 2019 we followed the outburst of this previously unknown BH X-ray transient. The source showed pronounced and fast variability/flaring activity in both the X-ray and optical bands, and became very bright, allowing accurate observations to be performed (e.g. Tucker et al. 2018; Shidatsu et al. 2018). After the discovery of the source, from April 2018 we started fast-optical photometric monitoring observations with IFI+Iqueye and Aqueye+ (Zampieri et al., 2018a,b; Fiori et al., 2018), in parallel with a campaign carried out in the X-ray band (in particular with the Swift and NICER telescopes; Bharali et al. 2019; Stiele & Kong 2020). We detected optical quasi-periodic oscillations (QPOs) in the power density spectrum, that match some of the QPOs observed in the X-rays, at three different epochs (Apr 2018, Jun 2018, Oct 2018), when the source was in the hard state (Fiori et al. 2021, in preparation). In addition, at all epochs, QPOs with a centroid consistent with half the frequency of the lower frequency X-ray QPO were observed. The Apr 2018 power spectra are shown in Figure 3.

Optical and/or infrared QPOs may be produced in different ways, directly from the inner disc or from a jet launched from the accretion disc (e.g. Veledina & Poutanen 2015; Malzac et al. 2018). Regardless of the specific mechanism, both the X-ray and optical fluxes are believed to be modulated at the Lense-Thirring (LT) precession frequency of the inner accretion disc (Stella & Vietri, 1998; Ingram et al., 2009). If the lowest modulation frequency is that observed in the optical power density spectrum, the characteristic precession frequency of MAXI J1820+070 is lower than that inferred from the 'fundamental' QPO in the X-rays (e.g. Stiele & Kong 2020), and this would indeed have important consequences for the

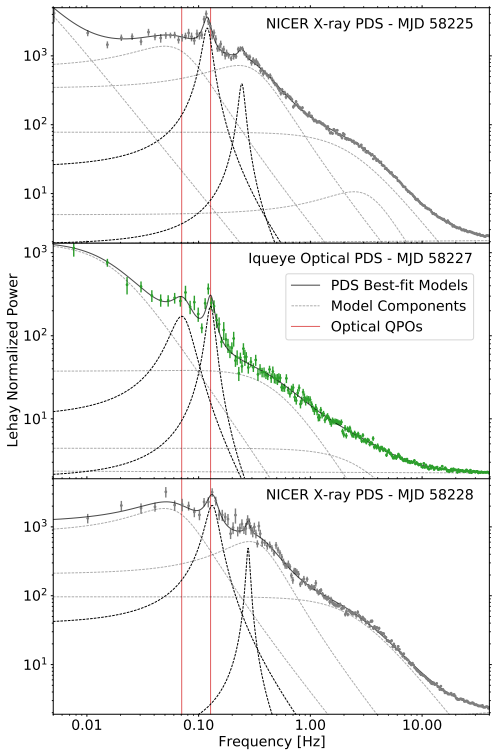

Fig. 3. Leahy normalized power density spectra of the BH X-ray transient MAXI J1820+070 in the X-ray and optical bands (Fiori et al. 2021). Top and bottom panels: power spectrum of NICER observations taken on MJD 58225 (Apr 17, 2018) and MJD 58228 (Apr 20, 2018), respectively. Mid panel: power spectrum of an IFI+Iqueye observation taken on MJD 58227 (Apr 19, 2018). The NICER observations bracket the IFI+Iqueye one. The black dashed lines show the QPOs, while the gray dashed lines other Lorentzian components used to fit the power spectrum. The red vertical lines mark the frequencies of the optical QPOs. The QPO at ~ 0.1 Hz is visible in all three power spectra and has an increasing centroid frequency. In addition, a broader QPO with a centroid consistent with half the frequency of the lower frequency X-ray QPO is observed in the IFI+Iqueye power spectrum.

modelling of the source and the determination of its fundamental physical parameters.

2.3. Jet variability in BH binaries

Decades of studies have shown that accretion on black holes is extremely turbulent, with characteristic timescales ranging from years down to milliseconds discovered in the radiation emitted by the infalling matter. Members of our collaboration have held a key leading role in studying this variable emission, proposing what is the currently favoured model for interpreting the fastest features (Stella & Vietri, 1998; Ingram et al., 2009; Veledina et al. , 2013), and contributing to the observational scenario with studies on single sources and classification efforts (Casella, Belloni & Stella , 2005). In recent years, we have participated to - and in some cases led - key discoveries of similar variability patterns in the radiation emitted by matter ejected by accreting black holes (Casella et al. , 2010; Gandhi et al. , 2010, 2017). We have since been very active in studying this variable emission and its strong correlation with the emission from the inflowing matter. This includes carrying out state-of-the-art observations to characterise its properties, and participating to its physical modelling. Our recent works brought to the discovery of a nearly constant dumping timescale in the infrared emission from a jet (Vincentelli et al. , 2019), to the first characterisation of rapid variability in the radio emission from a jet (Tetarenko et al. , 2019, 2021), and to strong constraints to the misalignment between the jet and the accretion disk (Vincentelli et al. , 2019).

3. White-dwarf (WD) binaries

3.1. The massive WD + hot subdwarf binary HD 49798

Evolutionary models predict the existence of accretion-powered X-ray binaries in which the mass donor is a hot subdwarf, but only one such system is known. It is formed by a massive, rapidly spinning white dwarf (M = 1.28±0.05 $M_\odot$, P =13.2 s) accreting matter from the weak stellar wind of its sdO companion star HD 49798 (Mereghetti et al. , 2009). The properties of this system are quite different from those of all the other

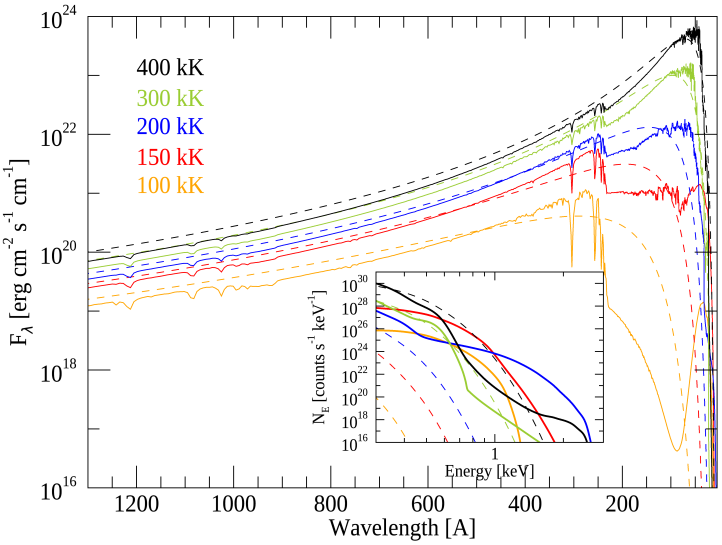

Fig. 4. Examples of our atmosphere model for different effective temperatures, compared to blackbody spectra (dashed lines). The model has been computed for a composition based on the element abundances of HD 49798 (assuming that the white dwarf is covered by matter accreted from its companion) and surface gravity log g = 9 (for details see Werner et al. 2012). The inset is a zoom in the 0.3-3 keV range, where the models have been convolved with the energy resolution of the *XMM-Newton* EPIC instrument.

known X-ray binaries. Its X-ray emission consists of a strongly pulsed soft thermal component (blackbody temperature kT∼30 eV) and a harder tail (power law photon index ∼2). The pulsar steady spin-up at a rate of -2.17×10^{-15} s s^{-1} (Mereghetti et al. , 2016), cannot be expained by accretion torques, while it is consistent with that expected for a young contracting white dwarf (Popov et al., 2018).

Mereghetti et al. (2021) recently computed the expected thermal emission for an atmosphere with element abundances and surface gravity appropriate for this massive white dwarf (Fig. 3.1) and used this model to fit its *XMM-Newton* X-ray spectra. The best fit was obtained with an effective temperature of T_{eff}=2.25×10^5 K and an emitting area with radius of ∼1600 km. This area is much larger than that previously found with blackbody fits (∼30 km). An important consequence of this more realistic modeling is that the contribution of the white dwarf pulsed emission in the optical band is significantly larger than previously thought. This is relevant for the modelling of the periodic modulation observed in the optical band from this system (with P_{orb}=1.55 d) and for the prospects of detecting the 13.2 s spin-period with fast optical photometry.

3.2. Symbiotic stars

We also explored, via multi-wavelength approach, a sample of symbiotic stars (SySt), that is, binary systems composed of a red giant orbited by an accreting WD. For long time the census of SySt has been dominated by systems with WDs burning nuclearly at their surface the accreted material. All-sky surveys and pointed X-ray observations (with the Swift satellite in particular) are now discovering their non-burning counterparts as optically inconspicuous red giants that emit hard X-rays and UV (e.g., Mukai et al. , 2016): so far, only a dozen such systems are known.

In detail, we have identified a first group of 33 new SySt candidates of the accreting-

only variety among the more than 600 000 stars so far observed by the GALactic Archaeology with HERMES (GALAH) high-resolution spectroscopic survey of the Southern hemisphere, thus more than doubling the number of those previously known (Munari et al. , 2021). The 33 new candidate SySt were subjected to an array of follow-up confirmatory observations (X-ray/ultraviolet monitoring, search for optical flickering, presence of a near-ultraviolet upturn in ground-based photometric and spectroscopic data, radial velocity changes suggestive of orbital motion, and variability of the emission-line profiles), and further multi-wavelength investigation of this sample is underway.

In Skopal et al. (2020) we instead focused on the case of star V426 Sge (HBHA 1704-05), which brightened at the beginning of August 2018 and showed signatures of a SySt outburst. To confirm the nature of V426 Sge as a classical SySt and to characterize the system properties, we reconstructed a historical light curve of the source from approximately year 1900, and used original low- and high-resolution optical spectroscopy complemented with Swift X-ray and ultraviolet data, as well as with optical and near-infrared photometry obtained during the 2018 outburst and the following quiescent state. Our spectral energy distribution modeling revealed that the donor is a normal M4-5 III giant characterised with $T_{\rm eff} \sim 3400$ K, radius $\sim$106 $R_\odot$ and luminosity $\sim$1350 $L_\odot$ (assuming a distance of 3.3 kpc), and that the accretor is a low-mass ($\sim$0.5 $M_\odot$) WD.

4. Neutron-star binaries

Accreting neutron-star binaries are subdivided into two main classes, low-mass X-ray binaries (LMXB) and high-mass X-ray binaries (HMXB), depending on the mass of the companion. Their properties are very different, not only because of the size of their orbits, but also because the neutron stars in HMXBs have a much higher magnetic field, which influences the accretion flow. Millisecond pulsars: they are a subset of LMXBs, in which the rotational period of the neutron star is observed directly as X-ray pulses. In particular, transitional millisecond pulsars are systems which show transition between a LMXB state, when they accrete from the companion, and a radio-pulsar state, when the emission is rotation-powered. Supergiant Fast X-ray Transients (SFXTs) are a subclass of HMXBs that, as the name suggests, contain a supergiant companion and are characterised by fast trasient behavior. Our work was focussed upon transitional millisecond pulsars, classical LMXBs and SFXTs.

4.1. Transitional millisecond pulsars

Millisecond pulsars (MSPs) are the quickest spinning neutron star known. We observe them as either radio pulsars powered by the rotation of the neutron star magnetic field or as accreting X-ray pulsars. Transitional MSPs can switch back and forth X-ray and radio pulsar states over a few days in response to variations of the mass accretion rate (Papitto et al. , 2013). Our group has been heavily involved in the efforts to increase the number of transitional MSPs (Coti Zelati et al. , 2019) and to characterize the emission mechanisms at work, both in the accretion (Papitto et al. , 2018) and in the rotation-powered (de Martino et al. , 2020) regime. Recently, the observation of transitional mode switching from an accreting white dwarf has provided a new environment to test the outcome of the disk/magnetic field interaction (Scaringi et al. , 2021). The reviews by Papitto & de Martino (2020) and Papitto et al. (2020) summarize the rich phenomenology observed and the main interpretative frameworks.

The fast optical photometer SiFAP2, operated at the Telescopio Nazionale Galileo and managed by members of our group widened the available probes of the physics of these systems. We discovered the first optical MSP in a transitional system (Ambrosino et al. , 2017). Simultaneous X-ray/optical observations proved that a single mechanism powers the pulsations observed in both bands, and that rotation and accretion powered regimes likely coexist (Papitto et al. , 2019) (see Figure 5). The subsequent discovery of an optical/UV signal from an accreting MSP (Ambrosino et al. , 2021) indicated that optical pulsars might

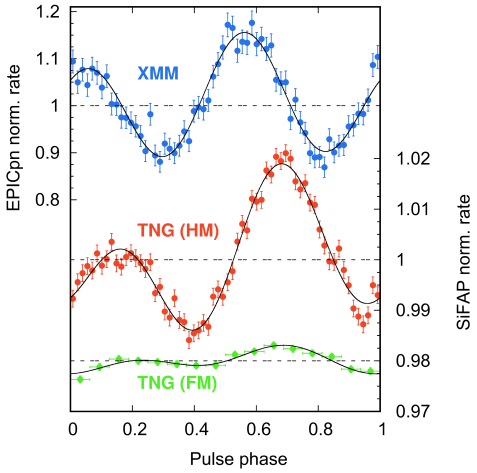

Fig. 5. Pulse profiles observed simultaneously by the ESA X-ray observatory XMM-Newton (blue points) and by the optical photometer SiFAP2 at the Telescopio Nazionale Galileo (red and green points) from the transitonal MSP PSR J1023+0038.

be more common than expected. Combined - often simultaneous - observations at X-ray energies and at other wavelengths (radio, optical, gamma-rays) played a crucial role in these studies and will allow us to explore the new discovery space opened by these findings.

4.2. Study of NS-LMXBs at several inclination angles

We investigated the orbital properties of MXB 1659-298. For our aim we used a baseline of 40 years obtained combining the eight eclipse arrival times present in literature with 51 eclipse arrival times collected during the last two outbursts (see Iaria et al. , 2018). Quadratic ephemeris are not enough to fit the delays associated with the eclipse arrival times and the addition of a sinusoidal term with a period of 2.31 ± 0.02 yr is required. We inferred a binary orbital period of $P = 7.1161099(3)$ hr and an orbital period derivative of $\dot{P} = -8.5(1.2) \times 10^{-12}$ s s^{-1}. The periodic modulation can be due to the presence of a third body of mass $M_3 > 21$ Jovian masses orbiting around the binary system.

During the outbursts in 1999 and 2015 MXB 1659-298 was observed by XMM-Newton, NuSTAR, and Swift/XRT. Using these observations, we studied the 0.45-55 keV broadband spectrum of the source to constrain the continuum components (Iaria et al. , 2019).We found that a reflection component is present in the soft and hard state. The direct emission in the soft state was modeled with a thermal component originating from the inner accretion disk plus a Comptonized component associated with an optically thick corona surrounding the NS. On the other hand, the direct emission in the hard state is described only by a Comptonized component with a temperature higher than 130 keV associated with an optically thin corona. The soft-state spectrum shows absorption lines from highly ionized ions of oxygen, neon, and iron. We inferred that the ionized absorber is distant 10^9 cm from the NS.

The dipping source XB 1916-053 is a compact binary system with an orbital period of 50 min harboring a NS. Using ten new Chandra observations and one Swift/XRT observation, we extended the baseline of the orbital ephemeris up to 40 years (Iaria et al. , 2021). From the analysis of the dip arrival times we determined an orbital period derivative of $P = 1.46(3) \times 10^{-11}$ s s^{-1} . The Chandra spectra show absorption lines associated with the presence of Ne x, Mg xii, Si xiv, S xvi and Fe xxvi ions. The lines show a redshift between 1.1×10^{-3} and 1.3×10^{-3}. By interpreting it as gravitational redshift we estimated that the ionized absorber is placed at a distance of 10^8 cm from the NS with a mass of 1.4 $M_\odot$.

We investigated the broadband spectrum of the ADC source X 1822-371 using XMM-Newton and NuSTAR observations. We found significant evidence of a reflection component in the spectrum, in addition to two narrow lines at 6.4 and 7.1 keV associated with neutral (or mildly ionized) iron. The continuum spectrum is well fitted by a saturated Comptonization model with an electron temperature of 4.9 keV and a thermal black-body-like component that might be emitted by the accretion disc at a lower temperature (0.2 keV). X 1822-371 is accreting at the Eddington limit with an intrinsic

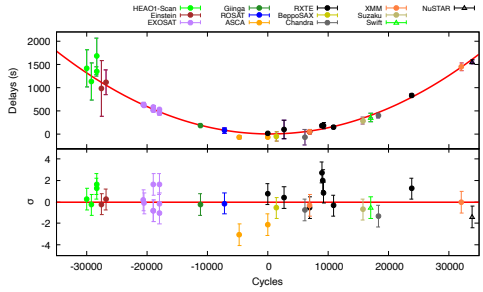

Fig. 6. Quadratic orbital ephemeris of X 1822-371 over 40 years. The corresponding values of orbital period and its derivative are shown in the text.

luminosity close to 10^{38} erg/s, while the observed luminosity is two orders of magnitude lower because of the high inclination angle of the system. Despite this high inclination, we find that a reflection component is required to fit residuals at the Fe line range and to model the hard excess observed in the NuSTAR spectrum (see Anitra et al. , 2021). We refined also the orbital ephemeris of X 1822-371 finding a stable orbital expansion over 40 years (Fig. 6), we found $P = 5.57063023(34)$ hr and a $P_{orb} = 1.51(5) \times 10^{-10}$ s s^{-1} (see Mazzola et al. , 2019; Anitra et al. , 2021).

Finally, we analyzed the NuSTAR spectrum of the bright source Sco X-1. We fitted the 3-60 keV NuSTAR spectra using the same models for Normal and Flaring branches. We adopted two description for the continuum: in the first case we used a blackbody and a thermal Comptonization with seed photons originating in the accretion disc; in the second one, we adopted a disc-blackbody and a Comptonization with a blackbody-shaped spectrum of the incoming seed photons. A power-law fitting the high energy emission above 20 keV was also required in both cases. Furthermore, two lines related to the Kα and Kβ transitions of the He-like Fe xxv ions were detected at 6.6 keV and 7.8 keV, respectively (Mazzola et al. , 2021).

4.3. Supergiant Fast X-ray Transients

At variance with the different types of X-ray binaries known since the early days of X-ray astronomy, SFXTs have been discovered relatively recently, that is, only in the last decade and a half. These systems usually host a neutron star orbiting around an early-type supergiant star (Negueruela et al. , 2006). In the X-ray band, they show a rather well-defined set of peculiar characteristics (see Sidoli , 2017, for a recent review) that were never seen in previously known classical supergiant X-ray binaries: (i) bright (~10^{36} erg s^{-1}) and fast (a few hours to a few days) X-ray transient behavior, (ii) high dynamic ranges of 10^3–10^5, and (iii) low duty cycles of 0.1–5% when observed above 20 keV. These properties challenge our understanding of the accretion processes onto neutron star compact objects and as such these sources are ideal and unique laboratories for theoretical models of accretion and associated observational phenomenology.

Specifically, we reported results from the analysis of XMM-Newton and INTEGRAL data of the SFXT IGR J16479−4514 (Sguera et al., 2020). During a XMM-Newton observation in 2012, no point-like X-ray emission was detected from the source; conversely, an extended X-ray halo was clearly detected up to a angular distance compatible with a dust-scattering halo produced by the X-ray source before being eclipsed by its companion donor star. The diffuse emission of the dust-scattering halo could thus be observed without any contamination from the central X-ray point source. Our comprehensive analysis of a previous XMM-Newton observation performed in year 2008 allowed us to clearly disentangle the scattering halo spectrum from the residual point-like emission; moreover, the latter could be separated into two components attributed to the direct X-rays from the source and to the ones scattered by the stellar wind.

From INTEGRAL data, we identified a very strong (~10^{-8} erg cm^{-2} s^{-1}) and fast (25 minutes duration) flare that was classified as a giant hard X-ray flare, since the measured peak luminosity is $7{\times}10^{37}$ erg s^{-1}. Giant X-ray flares from SFXTs are very rare; to date, only one has been reported from a different source (Romano et al., 2015). The giant flare from IGR J16479−4514 occurred at a specific orbital phase that has been previously suggested

to be linked to the presence of a stable large-scale structure in the supergiant wind. We invoked co-rotating interaction regions (CIRs) in the wind as a potential candidate for this phenomenon, and we proposed that the interaction of the compact object with such CIRs during its passage inside of them provided the very large amount of accreted material necessary to produce the exceptionally energetic hard X-ray flare.

5. The INTEGRAL Galactic Plane Scanning

The access to the Key INTEGRAL project *Keeping watch over our Galaxy* (GPS), and the Galactic Centre region observations, made possible to study not only LMXBs and HMXBs properties and behaviours but also allowed to perform one of the deepest and widest serendipitous hard X-ray surveys conducting a census of hard x-ray across the sky at energies ≥20 keV with high angular resolution that is essential in such crowded regions. Furthermore, by expanding time resolved maps at short timescale, a very productive search for transient X and Gamma-ray emitters was available resulting in about 200 new sources. In particular, almost all INTEGRAL surveys along the last 18 years, made use of the IBIS telescope providing the best combination of field of view, sensitivity and angular resolution with an energy response above 20 keV opening the obscure object to be detected and identified. These capabilities made possible a new view of the hard x-ray sky population since the 90ies when only the 37 sources observed with the SIGMA telescope in the 40-100 keV range were reported (Revnivstev M. et al. , 2004). The most recent result of this activity has been summarized in (Krivonos R.et al. , 2021).

Many different successful follow–up campaign using a multi-wavelength approach have been performed in order to classify the unidentified sources resulted from the IBIS and Swift survey. Recently we classify two poorly studied Galactic x-ray transient, namely IGR J20155+3827 and Swift J1713.4-4219, for which IBIS GPS data, new and/or archival X-ray and optical/NIR data allowed to pinpoint their nature. The IGR source is a distant HMXB while the Swift source is a LMXB (Onori F. et al. , 2021).

Using our tool to spot outburst from transient sources it has been possible then to report on quasi-simultaneous INTEGRAL, Swift and NuStar observation of the LMXB known as 1RXS J18048.9-342058 not only during its outburst in 2015 but also on a broad energy band (0.8-200 keV) in three different spectral states using archival data. Besides describing the spectral parameters in the high/soft, low/very hard and transitional states we have been able to classify it as a new clocked burster. In fact a 7.9ks average time between two successive burst has been detected with NuStar when the source was in the very hard state and 4ks at the time the source persistent emission decreased by a factor of 2 moving to transitional state. Decay time of bursts and accretion rate value of $\sim 4 \times 10^{-9} M_{\odot}/yr$ suggested the thermal emission as due to mixed H/He burning triggered by thermally unstable He ignition (Fiocchi M. et al. , 2019).

We also reported on a recent outburst from the binary transient MAXI J1631-479 detected during the GPS observation in January 2019. Two different spectral transitions between the high/soft and low/hard states have been studied (Fig. 7). Interestingly, the second transition was characterized by a hard power law spectrum indicating a non-thermal emission origin. Also, the outburst evolution in the hardness/intensity diagram, the spectral characteristic and the rise and decay time of the outburst are suggestive of a black hole as compact object.

The behaviour of the new microquasar MAXI J1820+070 has been monitored across the electromagnetic spectrum with detection from radio to hard X-ray frequencies with quasi-simultaneous observations along the outburst since 12 April 2018 onward. Hard x-ray data, flat/inverted radio spectrum and the accretion disk winds seen at optical wavelengths are consistent with the source being a black hole binary in the hard state. A spectral energy distribution spanning ∼12 orders of magnitude was constructed using modelling in `JetSeT` finding the spectrum dominated by jet emis-

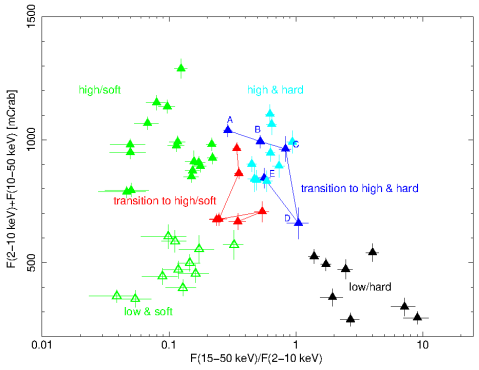

Fig. 7. The hardness-intensity diagram of MAXI J1631-479 with each point corresponding to 1 day: on the horizontal axis we show the ratio $F^{BAT}_{(15-50\,\mathrm{keV})}/F^{MAXI}_{(2-10\,\mathrm{keV})}$ and on the vertical axis the total flux $F^{BAT}_{(15-50\,\mathrm{keV})} + F^{MAXI}_{(2-10\,\mathrm{keV})}$. Colored points indicate the different time intervals. Capitals letters indicate the time evolution of the hardness-intensity data during this transition, with A being the starting of the transition and E the end.

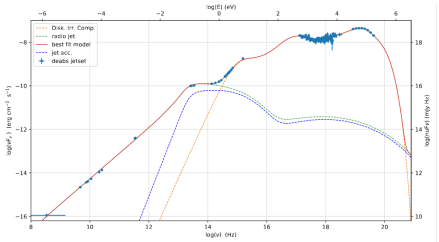

Fig. 8. The νF_ν representation of the Best-fit `JetSeT` model of the broadband SED. The red line represents the global model, the dashed lines correspond to the single components, the color is reported in the legend.

sion up to about 10^{14} Hz, after which disk and coronal emission dominate (see Fig. 8 and details in Rodi J. C., et al. 2021).

6. Accretion/ejection coupling in BH and NS X-ray binaries

Multi-wavelength spectral energy distributions (SEDs) of X-ray binaries (XRBs) with NS and BH during their hard spectral state are determined by the contribution of jets emitting from radio to mid-IR and the accretion flow (disk and corona) from optical to X-rays. Accretion and ejection appear as intimately different processes and yet, they seem to be deeply intertwined. However, the exact physical mechanisms underlying the coupling between matter inflows and outflows are still poorly understood.

The X-ray timing behaviour and spectra evolve between two main states: the hard state (HS) which is highly variable and dominated by the hard X-ray emission and the soft state (SS) less variable and characterized by a stronger contribution from the accretion disk. This dichotomy is usually explained in terms of changes in the accretion flow geometry (the disk is truncated in HS Done et al. 2007). At the same time, variability in the jets properties are also observed, even though similarities between BH and NS systems are less clear. BH systems in the HS launches a steady compact jet which is on the contrary quenched in the SS. This behaviour is observed sometimes also in NS systems (see, e.g. Gusinskaia et al. , 2017), even though in several cases radio jet are not quenched in SS (Migliari & Fender , 2006). In addition, radio jets in NS XRBs are less radio loud compared to those in BH systems (see, e.g. Gallo et al. , 2018).

4U 1820−30 is a NS XRB which periodically cycles between high and low X-ray accretion modes. Based on both radio and X-ray observation, we observed compact jet during the low X-ray modes which was quenched during the high X-ray modes (Russell et al. , 2021). We suggest that any changes in the boundary layer parameters and decrease of the inner disk radius (e.g., Gierlinski & Done , 2002), that are linked to the X-ray luminosity (i.e. the mass accretion rate), could be responsible for the jet changes (Fig. 9).

The Internal Shock Emission Jet model (ISHEM; Malzac 2014) assumes fluctuations in the velocity of the ejected shells along the jet driven by the fluctuations in the accretion flow. The jet model builds a simulated spectral energy distribution based on a wide set of physical parameters and on the X-ray Power Density Spectrum (PDS). The latter is used as a tracer of the fluctuations of the Lorentz factors in the ejected shells and the resulting inter-

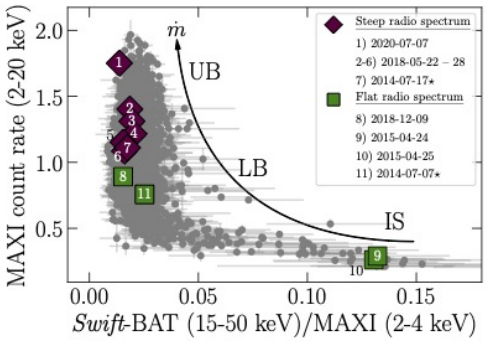

Fig. 9. Hardness intensity diagram of 4U 1820−30 (grey) along the super-orbital cycle. Magenta diamonds refer to radio observations corresponding to a quenched steady jet. Green squares mark observations where a steady jet is present (see details in Russell et al. , 2021).

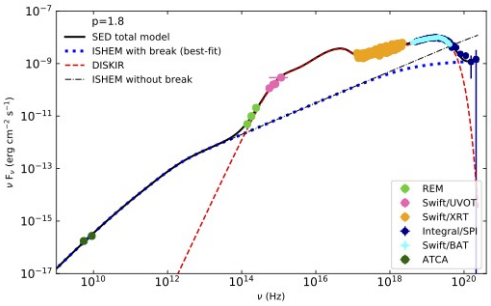

Fig. 10. Spectral energy distribution of GRS 1716−249. The MW data have been collected during a multi-wavelength (ATCA, REM, *Swift/XRT* and *INTEGRAL*) campaign performed in February-March 2017 (Bassi et al. , 2020).

nal shocks dissipation pattern. We have applied ISHEM for the first time to observations of a NS system, namely 4U 0614+091 (Marino et al. , 2020). Our results lead to two alternative scenarios: either a parabolic geometry should be invoked in NS XRBs, or the variability of the accretion flow is not strictly related to the jet shells. At present, it is unclear whether such observational differences may be connected to the presence of the NS magnetic field, to the spin and mass of the accretor, or to different properties of the accretion flow in NS compared to the BH systems.

We used ISHEM also to investigate the nature of the soft γ-ray emission above ∼150 keV observed in BH XRBs in hard state by the *INTEGRAL* satellite (e.g. Del Santo et al. , 2008; Bouchet et al. , 2009; Del Santo et al. , 2016). Usually, this component is explained in terms of Comptonisation process due to a non-thermal electron population in the corona (Coppi , 1999). However, based on polarization measurements of the Cyg X-1 emission above 250 keV, (Laurent et al. , 2011; Jurdain et al. , 2012) suggested synchrotron processes in the jet environment as possible origin of this component. Applying ISHEM to the MW data collected on the BH XRB GRS 1716–249 (Bassi et al. , 2019, 2020), we found that it is not possible to reproduce its soft γ-ray emission with the jet model, unless the index of the electron energy distribution would be lower than 2 (Fig. 10). However, slopes lower than 2 challenge the shock acceleration theory (Krymskii , 1977).

Recently a new paradigm, namely JED-SAD, (e.g. Ferreira et al. , 2006; Marcel et al. , 2018) to address accretion and ejection coupling has been proposed. This model is aimed at describing both the X-ray spectrum and the radio jet power emitted in hard state of BH XRBs. We applied JED-SAD to combined *NuSTAR*, *Swift/XRT* and NICER observations of the BH system MAXI J1820+070 in hard state (Marino et al. , 2021). We found that two Compton reflection components, likely associated to different regions of the accretion flow, are necessary to describe the X-ray spectra. One component is highly ionized and originating from the edge of the corona (JED), while the other is less ionized and possibly originates from the outer region of the disk (SAD). While the inner reflection component is stable, the outer one evolves compatibly with a scenario where the region responsible for such a component is approaching the BH. Thus, the geometry of the system consists in a truncated disk approaching towards the compact object along the evolution from the hard to the intermediate state.

Acknowledgements. We acknowledge financial contribution from the agreement ASI-INAF n.2017-14-H.0.

References

Ambrosino, F., et al., 2017, Nat. Astr., 1, 854
Ambrosino, F., et al., 2021, Nat. Astr., 5, 552
Anitra, A., et al., 2021, A&A, 654, A160
Bassi, T., et al., 2019, MNRAS, 482, 1587
Bassi, T., et al., 2020, MNRAS, 494, 571
Belloni, T.M., et al., 2020, MNRAS, 496, 4366
Bharali, P., Chauhan, J., & Boruah, K. 2019, MNRAS, 487, 5946
Bogensberger, D., et al., 2020, A&A 641 A101
Bouchet, L., et al., 2009, ApJ, 693, 1871
Casella, P., Belloni, T., Stella, L., 2005, ApJ, 629, 1
Casella, P., et al., 2010, MNRAS, 404, L21
Coppi, P. S., 1999, ASPC, 161, 375
Coti Zelati, F., et al., 2019, A&A, 622, A211
Del Santo, M., et al., 2008, MNRAS, 390, 227
Del Santo, M., et al., 2016, MNRAS, 456, 3585
de Martino, D., et al., 2020, MNRAS, 492, 5607
Done, C., et al., 2007, A&ARv, 15, 1
Ferreira, J., et al., 2006, A&A, 447, 813
Fiocchi M. et al., 2020, MNRAS, 492, 3
Fiocchi M. et al., 2019, ApJ, 887, 30
Fiori, M., et al. 2018, ATel, 11824
Gallo, E., et al., 2018, MNRAS, 478, 132
Gandhi, P., et al., 2010, MNRAS, 407, 2166
Gandhi, P., et al., 2017, Nat. Astr., 1, 859
Garcia, F., et al., 2021, MNRAS, 501, 3173
Gierlinski, M., & Done, C., 2002, MNRAS, 337, 1373
Gusinskaia, N., et al., 2017, MNRAS, 470, 1871
Iaria R., et al., 2018, MNRAS, 473, 349
Iaria R., et al., 2019, A&A, 630, A138
Iaria R., et al., 2021, A&A, 646, A120
Ingram, A., Done, C., & Fragile, P.C. 2009, MNRAS, 397, L101
Ingram, A.R., Motta, S.E., 2019, New Astronomy Reviews, 85, 10524
Jourdain, E., et al., 2012, ApJ, 761, 27
Karpouzas, K., et al., 2020, MNRAS, 492, 1399
Karpouzas, K., et al., 2021, MNRAS, 503, 5522
Krivonos R.et al., 2021, New Astronomy Reviews, 92, 101612
Krymskii, G. F., 1977, DoSSR, 234, 1306
Laurent, P., et al., 2011, Science, 332, 438
Malzac, J., 2014, MNRAS, 443, 299
Malzac, J., et al. 2018, MNRAS, 480, 2054
Marcel, G., et al. 2018, A&A, 615, 57
Marino, A., et al. 2020, MNRAS, 498, 3351
Marino, A., et al. 2021, A&A, 656, 63
Mazzola, S.M., et al., 2019, A&A, 625, L12
Mazzola, S.M., et al., 2021, A&A, 654, A102
Méndez, M., et al., 2021, Nature Astr., submitted
Mereghetti S., et al., 2009, Science, 325, 1222
Mereghetti S., et al. 2016, MNRAS, 458, 3523
Mereghetti S., et al., 2021, MNRAS, 504, 920
Migliari S. & Fender R., 2006, MNRAS, 366, 79
Mukai K., et al., 2016, MNRAS, 461, L1
Munari U., et al., 2021, MNRAS, 505, 6121
Negueruela, I., Smith, D., Reig, P., et al., 2006, in ESA SP-604, Proc. of the X-ray Universe 2005, ed. A. Wilson (Noordwijk: ESA), 165
Onori F. et al., 2021, MNRAS, 503, 472
Papitto, A., de Martino, D., 2020, arXiv:2010.09060
Papitto, A., et al., 2013, Nature, 501, 517
Papitto, A., et al., 2018, ApJL, 858, L12
Papitto, A., et al., 2019, ApJ, 882, 104
Papitto, A., et al., 2020, New Astr. Rev., 91, 10544
Popov S. B., et al., 2018, MNRAS, 474, 2750
Revnivstev M. et al., 2004, Astron. Lett. 30, 527–533
Rodi J. C., et al., ApJ, 2021, 920, 21
Romano, P., Bozzo, E., Mangano, V., et al. 2015, A&A, 576, L4
Russell, T. D. , et al. 2021, MNRAS, 508L, 6
Scaringi, S., et al., 2021, Nat. Astr., in press (arXiv:2110.09124)
Sguera V., et al. 2020, ApJ, 900, 22
Skopal A., et al., 2020, A&A, 636, A77
Shidatsu, M., et al. 2018, ApJ, 868, 54
Sidoli, L., 2017, in Proc. XII Multifrequency Behaviour of High Energy Cosmic Sources Workshop (Trieste: SISSA), 52
Stella, L. & Vietri, M. 1998, ApJL, 492, L59
Stiele, H. & Kong, A.K.H. 2020, ApJ, 889, 142
Tetarenko, A.J., et al., 2019, MNRAS, 484, 2987
Tetarenko, A.J., et al., 2021, MNRAS, 504, 3862
Tucker, M.A., et al. 2018, ApJL, 867, L9

Veledina, A., Poutanen, J., Ingram, A., 2013, ApJ, 778, 165
Veledina, A. & Poutanen, J. 2015, MNRAS, 448, 939
Vincentelli, F.M., et al., 2019, ApJL, 887, L19
Vincentelli, F.M., et al., 2021, MNRAS, 503, 614
Werner K., et al. 2012, TMAP: Tübingen NLTE Model-Atmosphere Package, Astrophysics Source Code Library [record ascl:1212.015]
Zampieri, L., et al. 2018, ATel, 11723
Zampieri, L., et al. 2018, ATel 11936
Zampieri, L., et al. 2019, Contributions of the Astronomical Observatory Skalnate Pleso, 49, 85
Zhang, L., et al., 2020, MNRAS, 494, 1375